

# Visual Analysis of Strapdown Inertial Navigation Information Model

Liwei Guo  
Xian E-Fly Avionics Science and  
Technology Company Shanxi  
Xian , 710000, China

Lei Wang\*  
Xian E-Fly Avionics Science and  
Technology Company Shanxi  
Xian , 710000, China

Wei Song  
Xian E-Fly Avionics Science and  
Technology Company Shanxi  
Xian , 710000, China

**Abstract:** Visual analysis of strapdown inertial navigation information model is studied in this paper. With the increasing demand for the accuracy of strapdown inertial navigation, gravity disturbance becomes the largest residual error of high-precision inertial navigation system. In this paper, the gravity disturbance is quantitatively analyzed according to the intelligent fusion spherical harmonic model. It is then equivalent to the resolution of high-precision acceleration and is a main error source of high-precision inertial navigation system. The Terrain system in Cesium is a technology that also supports the generation of terrains from streaming tile data. It supports two types of terrains, STK WorldTerrain and Small Terrain. We then test the combinations of the mentioned models.

**Keywords:** Visual Analysis ; Strapdown Inertial Navigation; Information Model; Data Mining

## 1. INTRODUCTION

In the strapdown inertial navigation system, the calculation accuracy of the carrier attitude will directly affect the system navigation accuracy [1, 2, 3]. Therefore, improving the calculation accuracy of the carrier attitude matrix is an important content of the strapdown inertial navigation system research. Due to the uncertainty of the motion process of the carrier and the non-exchangeability of the limited rotation of the rigid body, the existing attitude algorithm of the core strapdown inertial navigation system will introduce a non-exchangeable error, and reducing the core non-exchangeable error is an effective method to improve the attitude accuracy of the carrier [4, 5, 6].

The inertial device error is generally divided into two parts: constant value drift and random drift [7, 8, 9, 10]. The inertial device constant value error can be effectively compensated, but it will gradually change with time, and the constant value drift will not change every time the inertial navigation system is started. The SINS update algorithm can usually be divided into three parts: attitude, velocity and position update, and the attitude update algorithm is the core, and its solution accuracy affects the navigation accuracy of the entire core SINS system. The existing framework obtains the inertial data output of the carrier by simulating the motion trajectory of the carrier, superimposes the error noise of the inertial device, and iteratively calculates the attitude, speed and position of the object according to the known initial state.

Second-order damping loop, introducing external height information for negative feedback, so as to then realize the positioning of general strapdown inertial navigation. In the SINS/RCNS integrated navigation system, the core indirect sensitive horizon method of starlight refraction is used to obtain high-precision horizon information, and the refraction apparent height obtained by refraction is introduced into the system measurement, and the navigation error caused by the accelerometer offset is corrected. The figure 1 shows the core structure of the ground truth system.

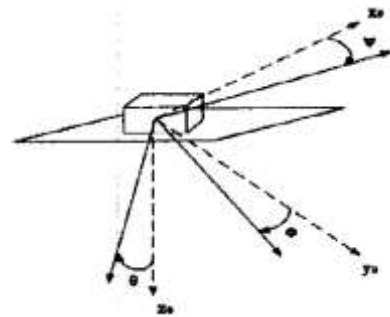


Figure. 1 The Ground Truth of System

For better efficient system construction, the combination of the information system is essential. With the development of science and technology and the continuous improvement of numerical simulation, computer graphics, computer vision, virtual reality and other technical means, the traditional static display can no longer meet the visual needs of the scientific visualization in various fields [11, 12, 13]. The vigorous development of Internet Web technology has provided a brand-new bearing platform for the GIS applications, and launched a brand-new WebGIS technology. Web-GIS uses the Internet as a carrier to reasonably express GIS-related functions, so that GIS services are widely popularized. Users can use GIS service functions as long as they have a device that can connect to the Internet. Hence, with this model, in the following sections, the general model will be defined and studied.

## 2. THE RELATED WORK

The Cesium as the visual analysis tool is reviewed in this section. The development process of Web 3D has evolved from the early Java Applet to plug-in Flash, Java3D, X3D, Silverlight, to plug-in-free WebGL, and then to the latest 3D graphics engine that encapsulates some common functions of 3D graphics programs [14, 15]. Cesium.js is an open-source front-end JavaScript library that can realize 2D, 2.5D and 3D data visualization on the Web side without plug-ins. It has good compatibility and interactivity for cross-platform browsers and multi-terminal devices. Compared with general WebGL, its development efficiency is higher, the amount of code writing is less, and it has powerful 3D rendering

functions. 3D Tiles is a 3D model tile data structure created by the Cesium R&D team to transmit massive heterogeneous 3D geospatial datasets [16, 17].

The Terrain system in Cesium is a technology that also supports the generation of terrains from streaming tile data. It supports two types of terrains, STK WorldTerrain and Small Terrain. AGI provides ready-made STK WorldTerrain data. For users with convenient network access, this data is the preferred solution [18, 19]. For users with limited access, they can choose to use tools to generate Small Terrain from ready-made DEM data slices to ensure terrain data loading.

### 3. THE PROPOSED METHODOLOGY

#### 3.1 The Data Visualization Model

Building profile data and height data are the basis for building modeling. In general SketchUp software, push-pull processing can be performed according to the estimated height and the appearance characteristics of the building to construct the model details of the building. In the modeling process, the method of creating components in the software can quickly improve the work efficiency [20, 21].

For buildings with the same appearance, the buildings can be built one by one and saved in SKP format, and finally imported into the model file uniformly. Cesium supports loading 3D models, and supports both gltf format and bgltf format. gltf is an exchange format defined by the Khronos organization, used to display 3D content on the Internet or mobile devices, and fully supports the OpenGL, WebGL, OPENGLES graphics acceleration standards; bgltf is a binary format gltf extension, its binary format reduces the size of the data, Improved network transfer speed [22, 23, 24].

We consider listed focuses.

(1) In practical applications, the point query function is the most commonly used function, which can quickly locate the position of the control point and query related attribute information. Therefore, the query function is particularly important. The system uses the ArcGIS server to publish data services, so it is very convenient to introduce the ArcGIS API for JavaScript development kit into the system to query data. Esri provides us with the Query Task class, which can realize the query of attribute data, obtain the location of the geometric elements and other related attribute information, and pass it to Cesium to finally realize the geographic positioning of geometric elements and realize the query function.

(2) The process of the projection texture mapping is to calculate the texture coordinates matching each vertex in the model through spatial projection transformation according to the physical parameters of the projection camera, such as spatial position, projection angle, coordinate information, etc., and to find the corresponding texture through the texture coordinate index [25].

(3) At present, spatial 3D model visualization is mostly based on professional software platforms, such as ArcScene, SuperMap, Skyline, etc. These methods have good spatial analysis functions and also display 3D data well, but the disadvantage is that it is not easy to share across platforms, and the cost is high. The 3D model visualization method of the /S framework is convenient for users to operate across servers, and the model rendering effect is relatively better. In the figure 3, the processing circle is defined.

#### 3.2 The Strapdown Inertial Navigation

After adding a damping network to the horizontal loop of the strapdown inertial navigation system, the Schuler period oscillation of the system can be damped, but the Schuler loop of the system is destroyed, which increases the error of the system. In order to overcome the error generated after the introduction of damping, the usual practice is to introduce external velocity information for the compensation, so as to achieve the purpose of both damping and compensating the errors caused by the acceleration and speed of the system. We follow the listed steps for the optimization [26, 27].

The modulation degree of the core positioning error represents the modulation degree of the rotation modulation technology to the positioning error. The larger the value, the better the modulation effect; on the contrary, the smaller the value, the less obvious the modulation effect is.

The positioning error of the general long time rotating strapdown inertial navigation system is mainly measured by the longitude error, while the latitude error oscillates with time but does not diverge.

The longitude error under the static condition of the strapdown inertial navigation system in the definition is the longitude error of the system when the indexing mechanism of the rotary strapdown inertial navigation system does not perform any action, that is, the system is in a static condition.

For the model design, the formula 1~3 define the calculation models.

$$L_{est} = \frac{V_n}{(R_0 + h)} \quad (1)$$

$$\lambda = \frac{V_e \sec L}{(R_0 + h)} \quad (2)$$

$$h = -V_d \quad (3)$$

After the error compensation calculation, the attitude matrix is calculated to obtain the attitude information; the accelerometer component measures the acceleration signals along the three axes of the carrier coordinate system, and after the error compensation calculation, the coordinate transformation calculation from the carrier coordinate system to the navigation coordinate system is performed. Realize navigation Precise demodulation after solving to obtain real carrier navigation information.

Therefore, the rotation accuracy of the rotating ring frame is an important index to ensure the accuracy of the dual-axis rotary inertial navigation system. The main errors of the rotating ring frame are introduced below. For the calibration of inertial device error parameters, the commonly used methods mainly include discrete calibration and system-level calibration. A large number of literatures give detailed research steps and research results for these two methods. This chapter studies an accurate modeling method of error parameters using artificial fish swarm algorithm. This method does not rely on high-precision testing equipment, and only needs to meet certain AFSA optimization indicators to achieve accurate fitting of each error coefficient. According to the differential equation (5.18) of the rotation angle of the rotation shaft, the rotation angle position of the rotation shaft can be obtained.

It can be seen from formula (5.18) that the rotation angle is affected by the motor voltage, inductance, resistance and other correlation coefficients, as well as the friction torque. At the same time, the assembly process has limitations, and the correlation coefficient is difficult to keep constant, which limits the stability and accuracy of the rotation angle control. Therefore, the essence of rotation modulation is to periodically change the value of the attitude matrix  $n_bC$ , so that  $n_{bb}C_\varepsilon$  and  $n$  The integral of  $bbCV$  in one rotation period is as close to zero as possible, so as to reduce the accumulation of system errors and improve the navigation accuracy. Assume that the IMU coordinate system at the initial time is the P system, the IMU rotating coordinate system is the R system, the IMU is installed on the carrier, the IMU coordinate system at the initial time coincides with the carrier system, and the IMU rotates continuously around the POz axis at an angular velocity  $\omega$ .

#### 4. THE SIMULATIONS

In our experiment, the system receives the synchronization signal command from the core time system module, and immediately sends the attitude data to the time system module. The data sent at this time is the attitude data that the system has already calculated, and there is a delay in the attitude transmitted to the time system module. In the case of navigation demand in a short period of time, the positioning of inertial navigation system is mainly composed of longitude error and latitude error. However, when the inertial navigation system needs to work for a long time, such as navigation and aviation, the latitude error oscillates with time, and the longitude error accumulates and diverges with time. Therefore, under the long-time working conditions, the divergence characteristics of longitude error are mainly considered to evaluate the positioning error of the system.

#### 5. CONCLUSIONS

Visual analysis of general strapdown inertial navigation information model is studied in this paper. The simulation analysis and experimental verification both show that the relevant theory of PEMD for the positioning error modulation of the rotary strapdown inertial navigation system is correct, so PEMD is an effective method to evaluate the positioning accuracy of the rotary strapdown inertial navigation system. Hence, this paper provides the novel solutions for the efficient model. In the future study, we will consider the applications.

#### 6. REFERENCES

[1]Hsu, Horng Yi, Yuichiro Toda, Kohei Yamashita, Keigo Watanabe, Masahiko Sasano, Akihiro Okamoto, Shogo Inaba, and Mamoru Minami. "Stereo-vision-based AUV navigation system for resetting the inertial navigation system error." *Artificial Life and Robotics* 27, no. 1 (2022): 165-178.

[2]Zhou, Zijun, Shuqin Yang, Zhisen Ni, Weixing Qian, Cuihong Gu, and Zekun Cao. "Pedestrian navigation method based on machine learning and gait feature assistance." *Sensors* 20, no. 5 (2020): 1530.

[3]Zhang, Chuang, Chen Guo, and Daheng Zhang. "Data fusion based on adaptive interacting multiple model for GPS/INS integrated navigation system." *Applied Sciences* 8, no. 9 (2018): 1682.

[4]Wan, Miao, Zhongbin Wang, Lei Si, Chao Tan, and Hao Wang. "An initial alignment technology of shearer inertial navigation positioning based on a fruit fly-optimized Kalman filter algorithm." *Computational Intelligence and Neuroscience* 2020 (2020).

[5]Wang, Guangqi, Yu Han, Jian Chen, Shubo Wang, Zichao Zhang, Nannan Du, and Yongjun Zheng. "A GNSS/INS integrated navigation algorithm based on Kalman filter." *IFAC-PapersOnLine* 51, no. 17 (2018): 232-237.

[6]Du, Binhan, Zhifei Ke, Yuan Zhu, Jianbin Su, and Zhiyong Shi. "Performance analysis for the model-aided inertial navigation system with different vehicle models." *Journal of the Brazilian Society of Mechanical Sciences and Engineering* 44, no. 3 (2022): 1-13.

[7]Cortés, Santiago, Arno Solin, and Juho Kannala. "Deep learning based speed estimation for constraining strapdown inertial navigation on smartphones." In *2018 IEEE 28th International Workshop on Machine Learning for Signal Processing (MLSP)*, pp. 1-6. IEEE, 2018.

[8]Chen, Kai, Jun Zhou, Fu-Qiang Shen, Han-Yan Sun, and Hao Fan. "Hypersonic boost-glide vehicle strapdown inertial navigation system/global positioning system algorithm in a launch-centered earth-fixed frame." *Aerospace science and technology* 98 (2020): 105679.

[9]Shen, Kai, M. S. Selezneva, and K. A. Neusypin. "Development of an algorithm for correction of an inertial navigation system in Off-Line mode." *Measurement Techniques* 60, no. 10 (2018): 991-997.

[10]Wang, Wei, and Xiyuan Chen. "Application of improved 5th-cubature Kalman filter in initial strapdown inertial navigation system alignment for large misalignment angles." *Sensors* 18, no. 2 (2018): 659.

[11]Li, Jinqiang, Jie Li, Li Qin, Wei Liu, Xiaokai Wei, Ning Gao, and Yang Liu. "Optimal design and analysis on high overload buffer structure of passive semi-strapdown inertial navigation system." *Sensors* 20, no. 4 (2020): 1131.

[12]Kaur, Amanpreet, Archana Mantri, and Vipin Kumar. "Design and development of mems sensors based inertial navigation systems for aerial vehicles: A case study." *International Journal of Sensors Wireless Communications and Control* 10, no. 2 (2020): 179-188.

[13]Guang, Xingxing, Yanbin Gao, Henry Leung, Pan Liu, and Guangchun Li. "An autonomous vehicle navigation system based on inertial and visual sensors." *Sensors* 18, no. 9 (2018): 2952.

[14]Sun, Yiding, Gongliu Yang, Qingzhong Cai, and Zeyang Wen. "A robust in-motion attitude alignment method for odometer-aided strapdown inertial navigation system." *Review of Scientific Instruments* 91, no. 12 (2020): 125006.

[15]Jao, Chi-Shih, Yusheng Wang, and Andrei M. Shkel. "Pedestrian inertial navigation system augmented by vision-based foot-to-foot relative position measurements." In *2020 IEEE/ION Position, Location and Navigation Symposium (PLANS)*, pp. 900-907. IEEE, 2020.

[16]Xiang, Zhiyi, and Jian Zhou. "An In-Motion Alignment Method for Laser Doppler Velocimeter-Aided Strapdown Inertial Navigation System." In *Advances in Precision Instruments and Optical Engineering*, pp. 323-334. Springer, Singapore, 2022.

[17]Wang, Zuocheng, and Xiaoxian Yao. "Adaptive Friction Compensation Control for a Roll-Isolated Strapdown Inertial Navigation System." In *Journal of Physics: Conference Series*, vol. 1905, no. 1, p. 012003. IOP Publishing, 2021.

- [18] Kalikhman, D. M., Kalikhman, L. Y., Grebennikov, V. I., Turkin, V. A., Akmaev, A. A., Nikolaenko, A. Y., & Gnusarev, D. S. (2018, May). Integrated approach to the development of digital regulators for inertial sensory elements of modern strapdown inertial navigation systems and of corresponding control software. In 2018 25th Saint Petersburg International Conference on Integrated Navigation Systems (ICINS) (pp. 1-4). IEEE.
- [19] Zbrutsky, Alexander, and Viktor Trunov. "Forecasting and Compensation of Random Drift of the Micromechanical Gyroscope as Sensors of Strapdown Inertial Navigation System." In 2020 IEEE 6th International Conference on Methods and Systems of Navigation and Motion Control (MSNMC), pp. 11-13. IEEE, 2020.
- [20] Jianzhong, Wang. "Research on initial alignment of vehicle strapdown inertial navigation system." *The Journal of Engineering* 2018, no. 16 (2018): 1629-1636.
- [21] Jing, Zhengyao, Jie Li, Xi Zhang, Kaiqiang Feng, and Tao Zheng. "A novel rotation scheme for MEMS IMU error mitigation based on a missile-borne rotation semi-strapdown inertial navigation system." *Sensors* 19, no. 7 (2019): 1683.
- [22] Petritoli, Enrico, and Fabio Leccese. "Navigation Equations, Uncertainty and Error Budget in Inertial Navigation Systems." In 2021 IEEE 8th International Workshop on Metrology for AeroSpace (MetroAeroSpace), pp. 376-380. IEEE, 2021.
- [23] Golovan, Andrey. "Inertial navigation in the Earth polar regions with using spatial quasi-coordinates." *Mathematics in Engineering, Science & Aerospace (MESA)* 10, no. 4 (2019).
- [24] Chen, Hua, Tarek M. Taha, and Vamsy P. Chodavarapu. "Towards Improved Inertial Navigation by Reducing Errors Using Deep Learning Methodology." *Applied Sciences* 12, no. 7 (2022): 3645.
- [25] Xu, Yuan, and Xiyuan Chen. "Online cubature Kalman filter Rauch–Tung–Striebel smoothing for indoor inertial navigation system/ultrawideband integrated pedestrian navigation." *Proceedings of the Institution of Mechanical Engineers, Part I: Journal of Systems and Control Engineering* 232, no. 4 (2018): 390-398.
- [26] Wu, Yuanxin, Chao He, and Gang Liu. "On inertial navigation and attitude initialization in polar areas." *Satellite Navigation* 1, no. 1 (2020): 1-6.
- [27] Ahmed, Dina Bousdar, and Kai Metzger. "Wearable-based pedestrian inertial navigation with constraints based on biomechanical models." In 2018 IEEE/ION Position, Location and Navigation Symposium (PLANS), pp. 118-123. IEEE, 2018.